# Influence of silver nanoparticles on the structure and mechanical properties of porous titanium nickelide alloys

***E. S. Marchenko***, *Doctor of Physical and Mathematical Sciences, Associate Professor, Head of the Laboratory of Medical Alloys and Shape Memory Implants*[1], *e-mail: 89138641814@mail.ru*
***G. A. Baigonakova***, *Candidate of Physical and Mathematical Sciences, Assistant, Senior Researcher*[1], *gat27@mail.ru*
***V. A. Larikov***, *Post-Graduate Student, Research Engineer*[1], *e-mail: calibra1995se@gmail.com*
***A. N. Monogenov***, *Candidate of Physical and Mathematical Sciences, Senior Researcher, Research Engineer*

[1]*National Research Tomsk State University, Tomsk, Russia.*

The aim of the work is to study the effect of silver doping on the structure and mechanical properties of porous titanium nickelide alloys obtained by self-propagating high-temperature synthesis (SHS). The structure of the samples was studied using *X*-ray diffraction analysis, scanning and transmission electron microscopy. The mechanical properties of porous alloys were studied in compression tests. An increase in the volume fraction of the B19' martensitic phase, intermetallic compounds based on the $Ti_2Ni$ and a decrease in the volume fraction of austenite with the B2 structure with an increase in the silver content were established. An increase in the plasticity of porous titanium nickelide alloys with an increase in the concentration of silver in the composition while maintaining the ultimate strength was revealed.

***Key words:*** porous titanium nickelide, silver nanoparticles, self-propagating high-temperature synthesis, microstructure, phase composition, mechanical properties.

***DOI:*** 10.17580/nfm.2022.02.13

## 1. Introduction

TiNi-based porous alloys are currently of high scientific and practical interest due to their ability to reversibly deform under physiological stress without destruction [1, 2]. A unique combination of the shape memory effect and superelasticity along with such technological and mechanical properties as strength and ductility, corrosion resistance, biocompatibility, allows using the alloys in medicine. The introduction of various alloying elements into the composition of titanium nickelide forms various structural and phase states and, as a result, influences efficiently the physical and mechanical characteristics, determined by these elements [3–5]. Titanium nickelide alloys with a porous structure are filled satisfactorily with tissue cells and biological fluids, which is promising when creating materials intended for osteoplasty [6, 7].

At present, when developing implants, special attention is paid to materials with antimicrobial activity to prevent infections [8]. Among the metals, silver is known for its antibacterial activity and low toxicity at certain concentrations. Silver has bactericidal activity at concentrations of up to 35 parts per billion without exerting toxic influence on mammalian cells [8, 9]. In addition, bacteria show a slight tendency to developing resistance to silver [9].

In the existing studies, the bulk of the works is devoted to studying the properties of monolithic titanium nickelide alloys with the addition of silver, and there are no studies on porous alloys based on titanium nickelide, obtained by the SHS method [10–20]. From the viewpoint of using TiNiAg materials in medicine, silver at a concentration from 0.5 to 9 at.% imparts new properties to the alloy, improving its cytocompatibility and antibacterial ability [10–14], while increasing the tensile yield stress and ultimate tensile strength [15, 16]. The shape memory effects of the Ag-doped TiNi were studied at a silver concentration of 1.4 at.% [11], while martensitic transformations, as well as microhardness, were mainly considered within 0.6–1.9 at.% of Ag [17–20]. Adding silver in the amount of up to 3 at. % was found to lead to an improvement in tribological properties, corrosion resistance and biocompatibility [23]. At a concentration of 0.7 at.%, the elastic modulus of the alloy corresponds to the spongy bone modulus and demonstrates satisfactory superelasticity at human body temperature [18]. Since the silver solubility in NiTi is very low, adding an excessive amount of silver leads to precipitation, making the composition heterogeneous and causing instability of the passive film. The studies of corrosion resistance and martensitic transformations allowed establishing the fact that the amount of silver, added to TiNi, should be within 0.5–1.5 at.% [11]. There were no studies devoted to the influence of the low silver content (<0.5 at.%) on the structure and mechanical properties of porous TiNiAg alloys, obtained by the SHS method.

Therefore, the purpose of the present research is to study the influence of silver doping on the structure and

physical-mechanical properties of porous titanium nickelide alloys, obtained by the SHS method.

## 2. Materials and research methods

The titanium nickelide powder of the PN45T55OM grade, nickel powder of the PNK OT-4 grade, titanium powder of the PTOM-2 grade and a silver nanopowder, having an average particle size of 8 nm, at concentrations of 0.2 at.% of Ag and 0.5 at.% of Ag were mixed together. For the more uniform mixing of the powders, silver and nickel were mixed first in the quantities that are similar in weight. Then the titanium powder was portionwise added and mixed, having coarser particles with a developed surface in comparison with nickel particles. The TiNiAg alloy samples were obtained by the SHS method when preliminarily charging the furnace with inert argon gas to prevent oxidation of the powders during heating. The synthesis was initiated by an electric arc, having previously maintained a stable temperature of 520 °C in the furnace. After conducting the SH-synthesis, the samples were cooled to room temperature by immersing them into water. The phase composition and structural parameters of the samples were studied using a Shimadzu XRD-6000 diffractometer in the Cu $K_\alpha$-radiation. The diffractograms were indexed be means of the PowderCell 2.4 full-profile analysis program and by comparing them with the PDF 4+ database. The images of the TiNiAg alloy surface were obtained using a scanning electron microscope with the Schottky cathode of Tescan MIRA 3 LMU (TESCAN ORSAY HOLDING, Brno, Czech Republic) equipped with an energy dispersive *X*-ray spectrometer of Oxford Instruments Ultim Max 40 (Oxford Instruments, High Wycombe, UK). The strength properties were studied by means of the Instron machine of the 5969 series (USA); a compression loading configuration was applied. The compression samples were cut out of the workpiece using the electrospark discharge machine and had geometric dimensions of 6′3′3 mm$^3$. When studying the mechanical properties of each composition, at least 5 samples were tested.

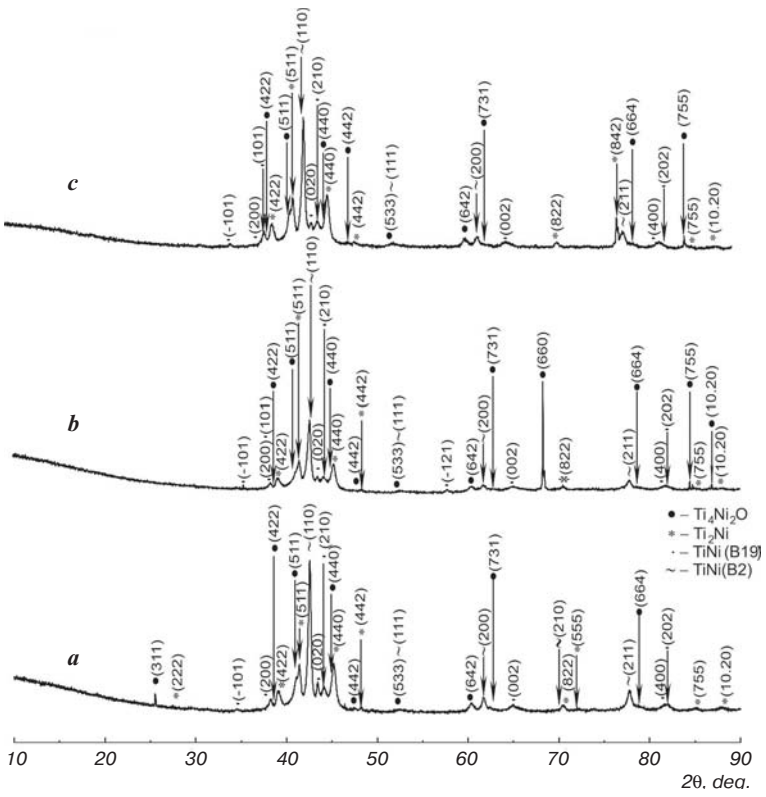


**Fig. 1.** *X*-ray diffractograms of TiNi porous SHS-alloy samples for: *a* – TiNi; *b* – TiNi + 0.2%Ag; *c* – TiNi + 0.5%Ag

## 3. Results and discussion

### 3.1. *X*-ray diffraction studies of TiNiAg alloys

**Fig. 1** shows *X*-ray diffractograms of the TiNi samples with the addition of Ag. The phase composition of the alloys under study is represented by $Ti_4Ni_2O$, $Ti_2Ni$, TiNi(B19'), TiNi(B2) phases. No Ag-based phases were detected probably owing to the small amount of silver.

The quantitative *X*-ray diffraction analysis of the TiNiAg alloys showed an increase in the volume fraction of the martensitic TiNi phase, having the B19' structure, and the growth of secondary phases, based on $Ti_2Ni$, $Ti_4Ni_2O$ compounds. It also demonstrated a decrease in the share of the austenitic TiNi phase, having the B2 structure, accompanied by an increase of the silver concentration in the alloy **(Fig. 2, *a*)**.

The dependence of the coherent scattering regions on the silver concentration shows that the crystallite size decreases for the TiNi phase, while it increases for $Ti_2Ni$. The CSR increase in the $Ti_2Ni$ phase is probably related to the fact that silver dissolves in the $Ti_2Ni$ phase; at the same time, silver is practically absent in the TiNi phase **(Fig. 2, *b*)**. Micro-distortions of the crystal lattices of all the intermetallic compounds, identified in the TiNiAg alloy system, were revealed by the quantitative *X*-ray structural analysis. This phenomenon is presumably associated with the fact that when increasing the silver concentration in the TiNi alloy, the lattice parameters of the TiNi(B19') and TiNi(B2) phases decrease, thereby changing the interatomic forces and increasing internal elastic stresses $\Delta d/d$ **(Fig. 2, *c*)**.

### 3.2. Scanning electron microscopy of TiNiAg porous SHS-alloys

The analysis of the porous macrostructure of the alloys showed that the porosity of all the samples did not depend on the silver concentration and it was equal to 62 ± 2% **(Fig. 3)**.

According to the histograms of the pore size distribution **(Fig. 4, *a*, *b*)**, when the silver concentration increased, the average pore size increased from 130 ± 9 to 168 ± ± 9 μm. The size of the interporous bridges also increased from 119 ± 10 to 145 ± 9 μm

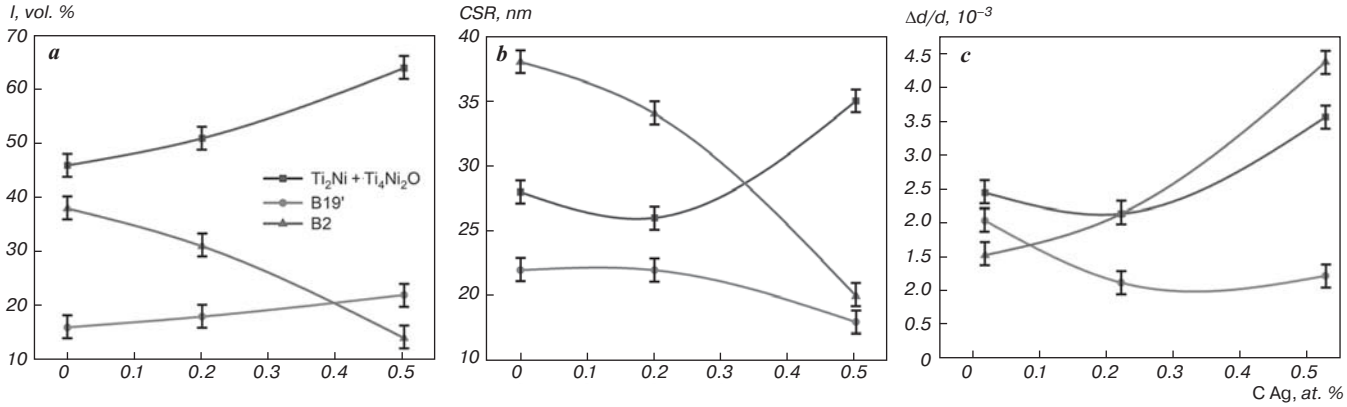


**Fig. 2.** Concentration dependence based on the results of the *X*-ray diffraction analysis of the samples of the TiNiAg porous SHS-alloy: *a* – volume fraction of phases; *b* – CSR values; *c* – micro-distortions

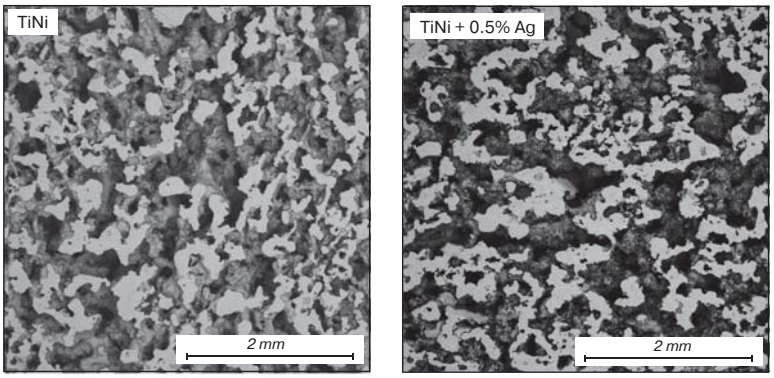


**Fig. 3.** Raster images of the sample surfaces of the TiNi porous SHS-alloy

**(Fig. 4, *c*, *d*)**. The sample size was about 200 measurements per sample. The average size of pores and brigdes was calculated by the random linear intercept method using ImageJ software.

The matrix of the TiNi porous SHS-alloy without the addition of silver consists of two phases. The first phase of gray color corresponds to the almost equiatomic composition of the TiNi compound in terms of the ratio between titanium and nickel. The dark gray inclusions are the intermetallic $Ti_2Ni(O)$ phase with the oxygen admixture, formed during the peritectic reaction **(Fig. 5, Table 1)**.

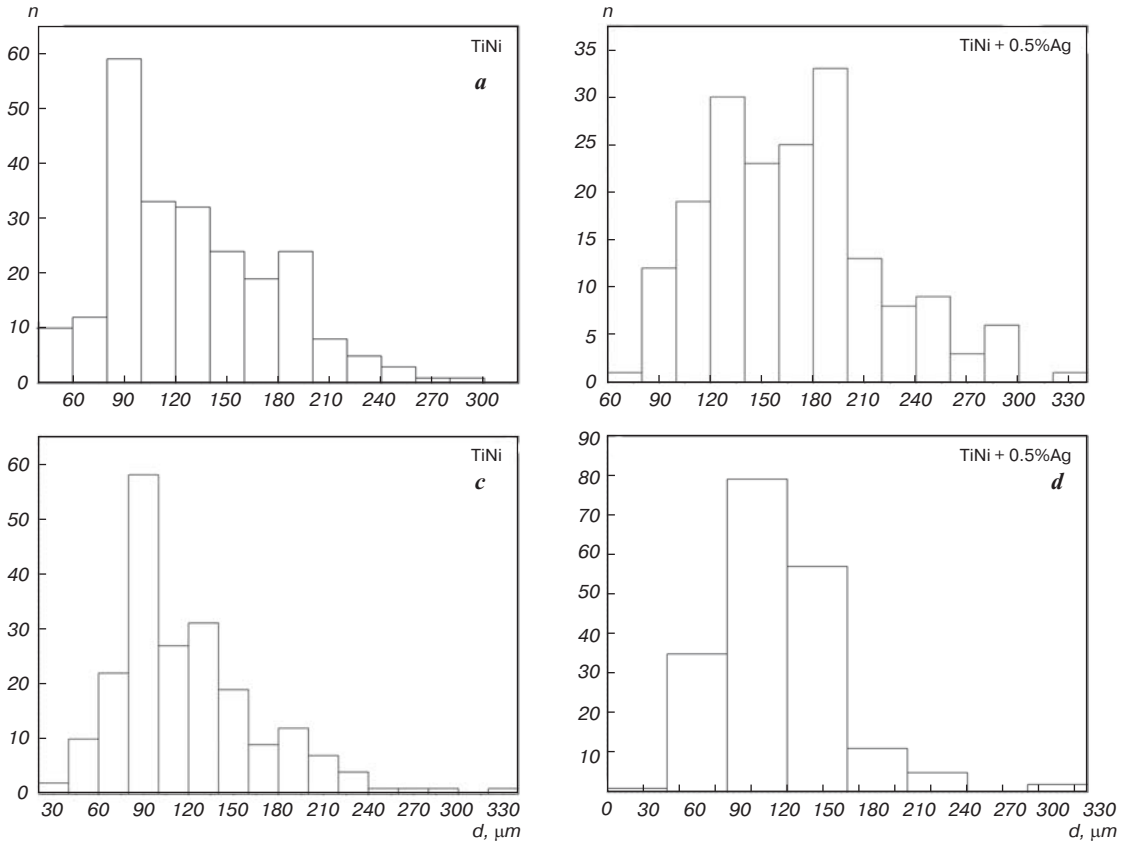


**Fig. 4.** Histograms of the size distribution of (*a*, *b*) – pores; (*c*, *d*) – interporous bridges in the samples of the TiNi porous SHS-alloy

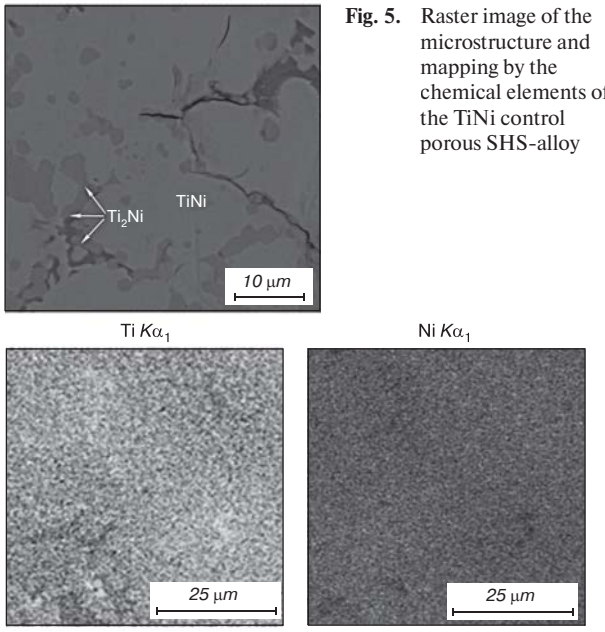


**Fig. 5.** Raster image of the microstructure and mapping by the chemical elements of the TiNi control porous SHS-alloy

Table 1
**Elemental composition of the phases in the TiNi porous SHS-alloy**

| Identification | Ti, at.% | Ni, at.% | O, at.% |
|---|---|---|---|
| TiNi (Ti and Ni alloy) | 49.36 | 50.64 | 0 |
| $Ti_2Ni$ | 56.2 | 36.87 | 6.93 |

Table 2
**Elemental composition of the phases in the TiNi + 0.2%Ag porous SHS-alloys**

| Identification | Ti, at.% | Ni, at.% | O, at.% | Ag, at.% | Ca, at.% |
|---|---|---|---|---|---|
| TiNi (Ti and Ni alloy) | 51.18 | 48.82 | – | – | – |
| $Ti_2Ni(O)$ | 59.55 | 29.84 | 10.09 | 0.52 | – |
| Ag | 0.41 | 0.29 | 4.23 | 89.06 | 6.01 |

SEM images and the corresponding element distribution maps for porous TiNi alloys at a silver concentration of 0.2 at.% and 0.5 at.% showed the presence of silver in the form of light particles up to 2 μm in size. The silver particles are to be noted to localize predominantly on $Ti_2Ni(O)$ or $Ti_4Ni_2O$ inclusions **(Figs. 6, 7; Table 2)**.

In some cases, silver was found to crystallize not only in pure form, but also in the form of coarse CaAg particles of up to 7 μm in size **(Fig. 8)**. The presence of calcium is associated with the method of obtaining the PTOM-2 titanium powder by means of hydride-calcium reduction. The elemental composition of the TiNiAg system shows that Ca was found only in silver particles **(Table 3)**.

Studies of the microstructure of the SHS-alloys of TiNiAg show that the silver solubility in the TiNi(B2) phase of the porous alloy is limited to 0.1 at.%. At the same time, other authors have found that the silver solubility in a cast alloy does not exceed 0.26 at.% [10, 11]. Ag is known to have a significantly different electronic structure with

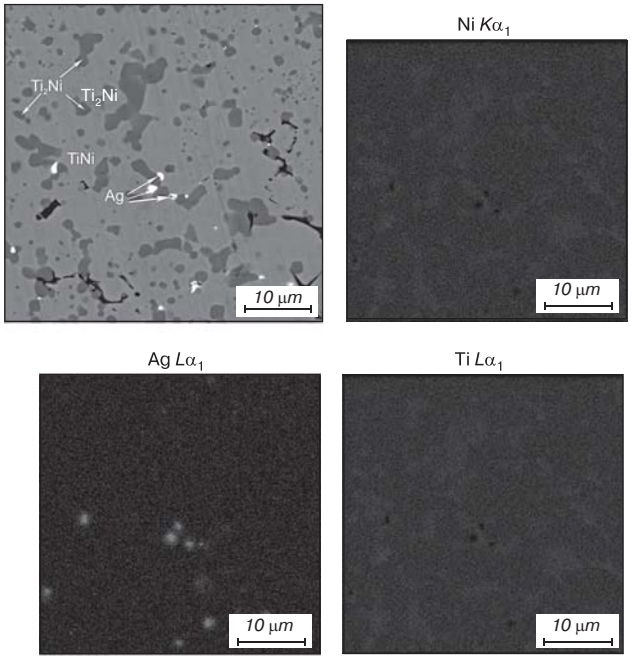


**Fig. 6.** Raster image of the microstructure and mapping by the chemical elements of the TiNi + 0.2%Ag porous SHS-alloy

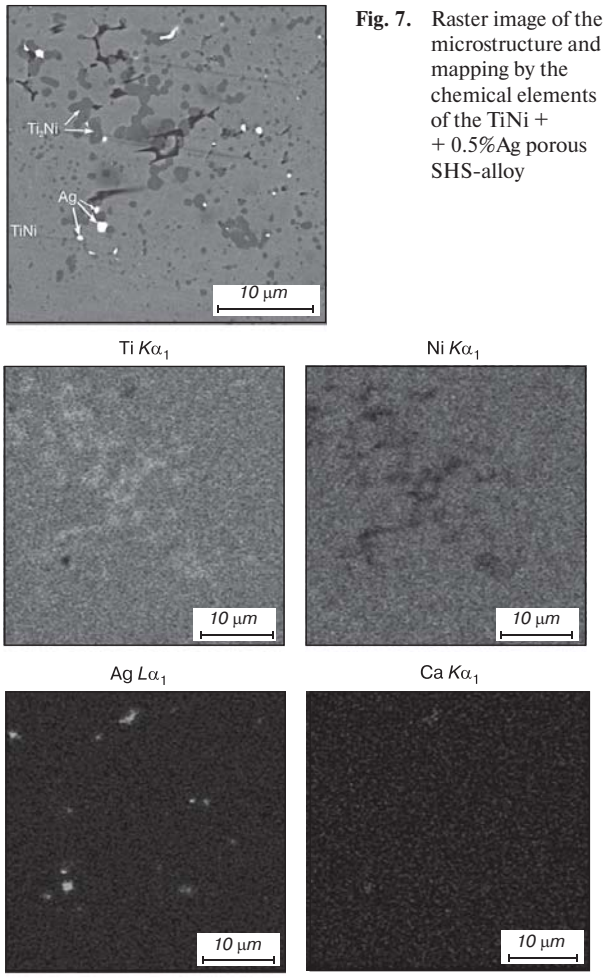


**Fig. 7.** Raster image of the microstructure and mapping by the chemical elements of the TiNi + + 0.5%Ag porous SHS-alloy

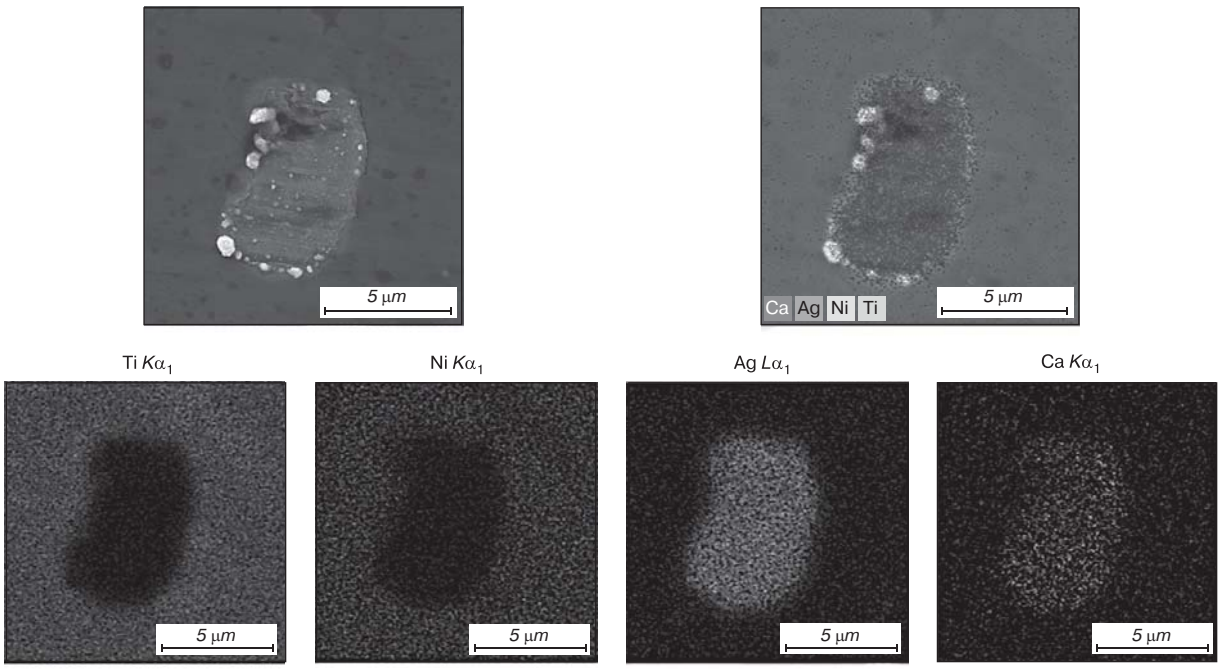


**Fig. 8.** Raster image of the microstructure and mapping by the chemical elements of the CaAg particle in the TiNi + 0.5%Ag porous SHS-alloy

reference to Ni and Ti elements from among three alloy-forming elements. In addition, Ag atoms vary significantly in size in comparison with Ni atoms. Therefore, the difference in the structure of the binary state diagrams of Ag – Ni, Ag – Ti and Ni – Ti systems is conditioned by the different structure of the electron atom shells of these three elements. The electronic subsystem behavior correlates with the phase diagrams of Ti – Ag binary alloys, where Ti and Ag in the Ti – Ag system can form solid solutions based on the initial components (Ag), (αTi), (αTi) and two intermetallic compounds AgTi и $AgTi_2$ at temperatures of 1020 ± 5 and 940 °C [22]. In the Ni – Ag system with a simple monotectic system in the state diagram, Ni and Ag are practically insoluble in each other. The maximum solubility of Ni in Ag is 0.102 at.%, and the maximum solubility of Ag in Ni is approximately 1 at.%, which decreases along with a decrease in temperature [4, 22].

The results of the energy dispersion spectroscopy analysis and mapping of the elements for the porous alloys at a silver concentration of 0.2 at.% and 0.5 at.% allow concluding that silver particles are localized mainly in the zones of peritectic crystallization of $Ti_2Ni(O)$ or $Ti_4Ni_2O$ inclusions. When the silver concentration in the alloy increases from 0.2% to 0.5%, the minimum, maximum and average particle size of pure silver increases **(Table 4)**.

### 3.3. Transmission electron microscopy of TiNiAg porous SHS-alloys

**Fig. 9** shows cross-sectional images of TiNiAg samples, obtained using a transmission electron microscope, which covers the areas of the surface layer and the matrix. The analysis results show that silver crystallizes in the form of nanoparticles up to 10 nm in size in the $Ti_4Ni_2O$ surface layer **(Fig. 9)**. One should note that silver crystallizes in the matrix in the form of coarse particles up to 2 μm in size. Similar data were obtained when studying ternary monolithic TiNiAg alloys, where silver was found only in the form of uniformly dispersed pure particles on the surface [10, 11]. In a number of other works, silver was found to be both in pure form and in the solid solution composition of the alloy-forming phases (silver solubility was 0.26 wt.%) [21, 18].

Table 3
**Elemental composition of the phases in SHS-alloys of TiNi + 0.5%Ag**

| Identification | Ti, at.% | Ni, at.% | O, at.% | Ag, at.% | Ca, at.% |
|---|---|---|---|---|---|
| TiNi (Ti and Ni alloy) | 51.2 | 48.73 | – | 0.1 | – |
| $Ti_2Ni(O)$ | 61.88 | 32.93 | 4.72 | 0.47 | – |
| Ag | 0.28 | 0.81 | 4.24 | 88.86 | 5.81 |

### 3.4. Mechanical properties of TiNiAg porous SHS-alloys

The mechanical properties of TiNiAg porous SHS-alloys were studied according to the compression loading configuration. When the silver concentration increased, the strength properties did not change, the ultimate strength was 74 ± 2 MPa **(Fig. 10, Table 5)**. The elastic strength decreases from 26 to 12 MPa, the elastic modulus decreases from 1700 to 950 MPa along with an increase of the silver content in the TiNi alloy. The maximum strain-to-fracture during compression of porous TiNiAg alloys increased from 7 to 27% along with an increase in the silver concentration. A similar effect on the mechanical characteristics was found in the studies on the influence

Table 4
**Statistical parameters of the size distribution of silver particles in TINiAg porous SHS-alloys**

| Sample | Min, μm | Max, μm | Average, μm | RSE | Dispersion |
|---|---|---|---|---|---|
| 0.2% Ag | 0.19 | 1.619 | 0.81 ± 0.11 | 0.281 | 0.07 |
| 0.5% Ag | 0.542 | 5.962 | 1.79 ± 0.45 | 1.113 | 1.23 |

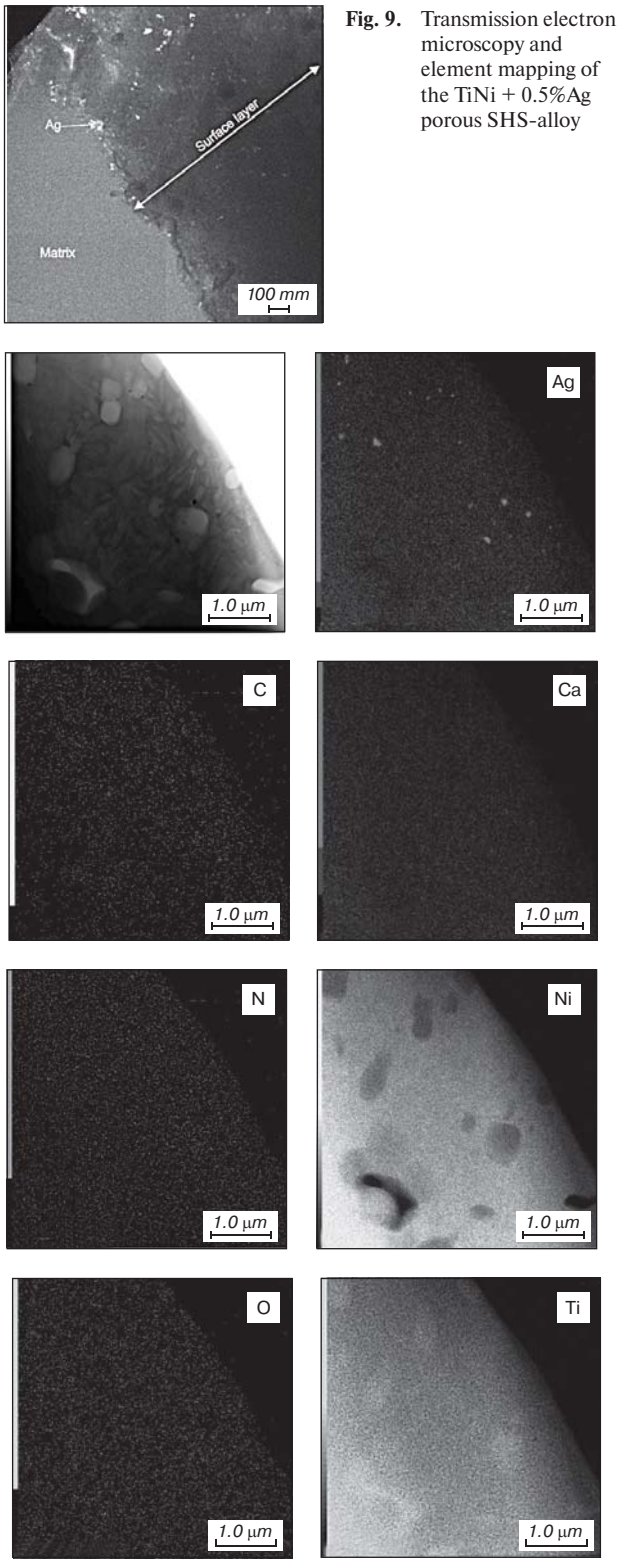


**Fig. 9.** Transmission electron microscopy and element mapping of the TiNi + 0.5%Ag porous SHS-alloy

Table 5
**Mechanical properties of TiNiAg porous SHS-alloys**

| Alloy | $E$, MPa | $\sigma_e$, MPA | $\sigma_{com}$, MPa | $\varepsilon_{com}$,% | $P$, % |
|---|---|---|---|---|---|
| TiNi | 1733 ± 10 | 26 ± 1 | 71 ± 2 | 7 ± 1 | 62 ± 2 |
| TiNi + 0.2%Ag | 1000 ± 12 | 15 ± 1 | 70 ± 4 | 16 ± 2 | 63 ± 2 |
| TiNi + 0.5%Ag | 958 ± 8 | 12 ± 2 | 74 ± 2 | 27 ± 2 | 62 ± 2 |

***Note:*** $E$ – elasticity modulus; $\sigma_e$ – elastic strength; $\sigma_{com}$ – ultimate compression strength; $\varepsilon_{com}$ – maximum deformation during compression up to destruction; $P$ – porosity.

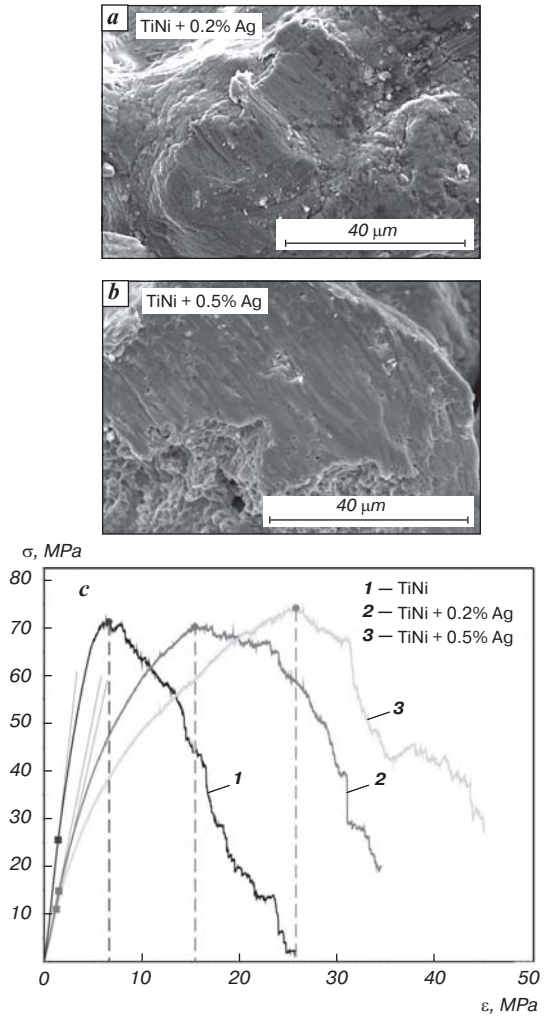


**Fig. 10.** Fracture surface image of the alloy sample for: *a* – TiNi + 0.2%Ag; *b* – TiNi + 0.5%Ag; *c* – dependence s-e for SHS-alloys of TiNiAg

of doping monolithic TiNi alloys with silver [4, 18]. The plasticity increase is apparently caused by the uniform distribution of silver nanoparticles, which, deforming plastically, hinder the crack propagation. Additional evidence of enhanced plastic properties is SEM images of fracture surfaces of porous TiNiAg alloys subject to compression testing, on which plastic shear traces are present.

The explanation of the significant enhancement of the plastic properties of porous TiNiAg alloys obtained by the SHS method requires a deeper and more comprehensive study.

## 4. Conclusion

The results of the conducted studies allow concluding that silver dissolves restrictedly in the TiNi(B2) phase up to 0.1 at.% and crystallizes in the form of pure silver particles or a small amount of the solid calcium solution in silver. Coarsely crystalline silver particles up to 2 μm in size were found in the matrix in the zones of peritectic crystallization of $Ti_2Ni(O)$ or $Ti_4Ni_2O$ inclusions. In the surface $Ti_4Ni_2O$ layer, silver particles crystallized uniformly in the nanocrystalline state up to 10 nm in size. An increase of the plastic properties from 7 to 27% was established along with an increase of the silver volume fraction; at the same time, the ultimate compression strength did not change and was 70±4 MPa. The physical and mechanical properties were at the level that is acceptable for practical application of porous TiNiAg alloys as an implantation material.

## Funding

***The research was carried out with financial support of the Russian Science Foundation under the Grant No. 22-72-10037, https://rscf.ru/project/22-72-10037/.***

## References

1. Otsuka K., Ren X. Physical Metallurgy of Ti -Ni-Based Shape Memory Alloys. *Progress in Materials Science*. 2005. Vol. 50, Iss. 5. pp. 511–678.

2. Eggeler G., Hornbogen E., Yawny A., Heckmann A., Wagner M. Structural and Functional Fatigue of NiTi Shape Memory Alloys. *Materials Science and Engineering: A*. 2004. Vol. 378, Iss. 1-2. pp. 24–33.

3. Monogenov A. N., Marchenko E. S., Baigonakova G. A., Yasenchuk Yu. F., Garin A. S., Volinsky A. A. Improved Mechanical Properties of Porous Nitinol by Aluminum Alloying. *Journal of Alloys and Compounds*. 2022. Vol. 918. 165617.

4. Baigonakova G. A., Marchenko E. S., Chekalkin T. L., Kang J., Weiss S., Obrosov A. Influence of Silver Addition on Structure, Martensite Transformations and Mechanical Properties of TiNiAg Alloy Wires for Biomedical Application. *Materials*. 2020. Vol. 13, Iss. 21. 4721.

5. Marchenko E. S., Baigonakova G. A., Gunther V. E. Effect of Alloying of Titanium Nickelide-Based Alloys with Group V Elements (Vanadium, Niobium) on Their Mechanical Properties. *Russian Metallurgy (Metally)*. 2018. Iss. 10. pp. 990–994.

6. Hornbogen E. Microstructure and Thermo-Mechanical Properties of NiTi Shape Memory Alloys. *Materials Science Forum*. 2004. Vol. 455-456. pp. 335–341.

7. Shen J.-J., Lu N.-H., Chen C.-H. Mechanical and Elastocaloric Effect of Aged Ni-Rich TiNi Shape Memory Alloy Under Load-Controlled Deformation. *Materials Science and Engineering: A*. 2020. Vol. 788. 139554.

8. Pratten J., Nazhat S., Blaker J., Boccaccini A. In Vitro Attachment of Staphylococcus Epidermidis to Surgical Sutures with and Without Ag-Containing Bioactive Glass Coating. *Journal of Biomaterials Applications*. 2004. Vol. 19, Iss. 1. pp. 47–57.

9. Chambers C., Proctor C., Kabler P. Bactericidal Effects of Low Concentrations of Silver. *Journal – American Water Works Association*. 1962. Vol. 54, Iss. 2. pp. 208–216.

10. Zheng Y., Zhang B., Wang B., Wang Y., Li L., Yang Q., Cui L. Introduction of Antibacterial Function into Biomedical TiNi Shape Memory Alloy by the Addition of Element Ag. *Acta Biomaterialia*. 2011, Vol. 7, Iss. 6. 2758–2767.

11. Oh K.-T., Joo U.-H., Park G.-H., Hwang C.-J., Kim K.-N. Effect of Silver Addition on the Properties of Nickel-Titanium Alloys for Dental Application. *Journal of Biomedical Materials Research Part B: Applied Biomaterials*. 2006. Vol. 76B, Iss. 2. pp. 306–314.

12. Li S., Kim Y.-W., Nam T.-H. Transformation Behavior and Superelastic Properties of Ti – Ni – Ag Scaffolds Prepared by Sintering of Alloy Fibers. *Scripta Materialia*. 2018. Vol. 153, pp. 23–26.

13. Momeni S., Tillmann W. Influence of Ag on Antibacterial Performance, Microstructure and Phase Transformation of NiTi Shape Memory Alloy Coatings. *Vacuum*. 2019. Vol. 164. pp. 242–245.

14. Jhou W.-T., Wang C., Ii S., Chiang H.-S., Hsueh C.-H. TiNiCuAg Shape Memory Alloy Films for Biomedical Applications. *Journal of Alloys and Compounds*. 2018. Vol. 738. pp. 336–344.

15. Gilberto H. T., da Silva Á., Otubo J. Designing NiTiAg Shape Memory Alloys by Vacuum Arc Remelting: First Practical Insights on Melting and Casting. *Shape Memory and Superelasticity*. 2018. Vol. 4, Iss. 4. 402–410.

16. Marchenko E. S., Baigonakova G., Gyunter V. E. The Effect of Silver Doping on the Structure and Shape Memory Effect in Biocompatible TiNi Alloys. *Technical Physics Letters*. 2018. Vol. *44*, Iss. 8. 749–752.

17. Chun S.-J., Noh J.-P., Yeom J.-T., Kim J.-I., Nam T.-H. Martensitic Transformation Behavior of Ti–Ni–Ag Alloys. *Intermetallics*. 2014. Vol. 46. pp. 91–96.

18. Li S., Kim E.-S., Kim Y.-W., Nam T.-H. Microstructures and Martensitic Transformation Behavior of Superelastic Ti –Ni – Ag Scaffolds. *Materials Research Bulletin*. 2016. Vol. 82. pp. 39–44.

19. Jang J.-Y., Chun S.-J., Kim N.-S., Cho J.-W., Kim J.-H., Yeom J.-T., Nam T.-H., Kim J.-I. Martensitic Transformation Behavior in Ti – Ni – X (Ag, In, Sn, Sb, Te, Tl, Pb, Bi) Ternary Alloys. *Materials Research Bulletin*. 2013. Vol. 48, Iss. 12. pp. 5064–5069.

20. Yi X., Pang G., Sun B., Meng X., Cai W. The Microstructure and Martensitic Transformation Behaviors in Ti – Ni – Hf – X (Ag, Sn) High Temperature Shape Memory Alloys. *Journal of Alloys and Compounds*. 2018. Vol. 756. pp. 19–25.

21. Zamponi C., Wuttig M., Quandt E. Ni–Ti–Ag Shape Memory Thin Films. *Scripta Materialia*. 2007. Vol. 56, Iss. 12. pp. 1075–1077.

22. Marchenko E. S., Baigonakova G. A., Kokorev O. V., Klopotov A. A., Iuzhakov M. M. Phase Equilibrium, Structure, Mechanical and Biocompatible Properties of TiNi-Based Alloy with Silver. *Materials Research Express*. 2019. Vol. 6, Iss. 6. 066559.

23. Thangavel E., Dhandapani V. S., Dharmalingam K., Marimuthu M., Veerapandian M., Arumugam M. K., Kim S., Kim B., Ramasundaram S., Kim D.-E. RF Magnetron Sputtering Mediated NiTi/Ag Coating on Ti-Alloy Substrate with Enhanced Biocompatibility and Durability. *Materials Science and Engineering: C*. 2019. Vol. 99. pp. 304–314.

NFM